Functional Characterization of a Novel BRCA1-Null Ovarian Cancer Cell Line in Response to Ionizing Radiation

Christiana DelloRusso,[1] Piri L. Welcsh,[1] Weixin Wang,[5] Rochelle L. Garcia,[2] Mary-Claire King,[1,3] and Elizabeth M. Swisher[1,4]

[1]Department of Medicine, Division of Medical Genetics; Departments of [2]Pathology, [3]Genome Sciences, and [4]Obstetrics and Gynecology, University of Washington, Seattle, Washington; and [5]Mary Babb Randolph Cancer Center, Department of Microbiology, Immunology and Cell Biology, West Virginia University, Morgantown, West Virginia

Abstract

The breast and ovarian cancer susceptibility gene *BRCA1* plays a major role in the DNA damage response pathway. The lack of well-characterized human BRCA1-null cell lines has limited the investigation of BRCA1 function, particularly with regard to its role in ovarian cancer. We propagated a novel BRCA1-null human ovarian cancer cell line UWB1.289 from a tumor of papillary serous histology, the most common form of ovarian carcinoma. UWB1.289 carries a germline *BRCA1* mutation within exon 11 and has a deletion of the wild-type allele. UWB1.289 is estrogen and progesterone receptor negative and has an acquired somatic mutation in *p53,* similar to the commonly used BRCA1-null breast cancer cell line HCC1937. We used ionizing radiation to induce DNA damage in both UWB1.289 and in a stable UWB1.289 line in which wild-type BRCA1 was restored. We examined several responses to DNA damage in these cell lines, including sensitivity to radiation, cell cycle checkpoint function, and changes in gene expression using microarray analysis. We observed that UWB1.289 is sensitive to ionizing radiation and lacks cell cycle checkpoint functions that are a normal part of the DNA damage response. Restoration of wild-type BRCA1 function in these cells partially restores DNA damage responses. Expression array analysis not only supports this partial functional correction but also reveals interesting new information regarding BRCA1-positive regulation of the expression of claudin 6 and other metastasis-associated genes and negative regulation of multiple IFN-inducible genes. (Mol Cancer Res 2007;5(1):35–45)

Received 7/31/06; revised 10/25/06; accepted 10/25/06.
Grant support: NIH grants R01 ES013160 (M-C. King) and T32 HD 007453 (C. DelloRusso) and Marsha Rivkin Center for Ovarian Cancer Research (P.L. Welcsh).
The costs of publication of this article were defrayed in part by the payment of page charges. This article must therefore be hereby marked *advertisement* in accordance with 18 U.S.C. Section 1734 solely to indicate this fact.
Note: M-C. King is an American Cancer Society Professor.
Requests for reprints: Elizabeth Swisher, Department of Medicine, Division of Medical Genetics, University of Washington School of Medicine, Seattle, WA 98195-7720. Phone: 206-616-7293. E-mail: swishere@u.washington.edu

doi:10.1158/1541-7786.MCR-06-0234

Introduction

Ovarian carcinoma is the fourth leading cause of cancer death in American women and has the highest mortality of the gynecologic cancers. Approximately 10% to 15% of ovarian carcinomas occur secondary to an inherited mutation in *BRCA1* or *BRCA2* (1, 2) Inherited mutations in *BRCA1* confer lifetime risks of breast cancer of 60% to 80% and of ovarian cancer of >25% to 50% (3, 4). A better understanding of the molecular events of ovarian transformation would facilitate improved surveillance, prevention, and therapy. Although recent advances have been made in developing mouse models for sporadic ovarian carcinoma (5-8), *in vitro* models for hereditary ovarian carcinoma are limited.

BRCA1 encodes a 1,863-amino-acid protein that associates with a multitude of proteins involved in cell cycle checkpoint regulation, DNA repair, transcription, chromatin remodeling, and ubiquitination (9-13), suggesting that BRCA1 plays a critical role in the cellular response to DNA damage. However, the exact mechanism by which BRCA1 functions in the DNA damage response is not completely understood, partly due to the paucity of human BRCA1-null cell lines available for study. Cellular models of hereditary ovarian cancer are especially lacking, with one ovarian endometrioid BRCA1-null cell line available for study (14), and two ovarian, papillary serous BRCA1-null lines recently developed from xenografts but not yet functionally characterized (15).

Ionizing radiation (IR) induces breaks in double-stranded DNA, the most severe DNA lesions that compromise genomic integrity if left unrepaired. Breaks in double-stranded DNA induce a robust DNA damage response that includes delays in cell cycle progression (induction of cell cycle checkpoints) and activation of DNA repair mechanisms (16, 17). Cell cycle checkpoints and DNA repair mechanisms are coordinated by multiple, complex signal transduction pathways and are highly dependent on the protein kinase function of the ataxia telangiectasia mutated (ATM) protein (18, 19). In response to DNA damage, ATM phosphorylates multiple proteins involved in cell cycle checkpoint regulation and DNA repair, including BRCA1 (20).

Our goal was to develop and characterize a unique BRCA1-null cell line to be used specifically to study BRCA1 function in ovarian cancer. In response to DNA damage induced by IR, our cell line (UWB1.289) lacks DNA repair and cell cycle checkpoint functions. We have also

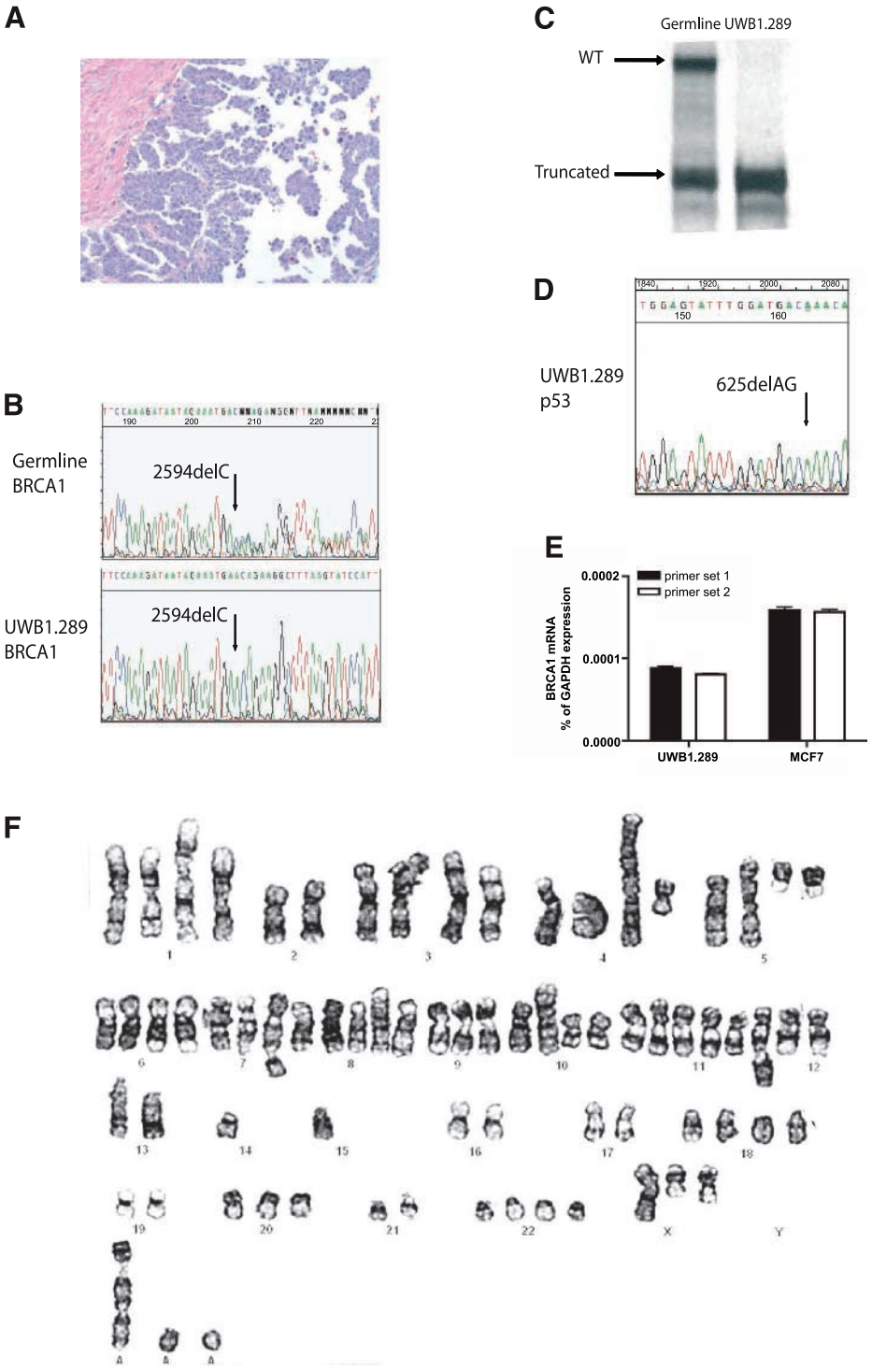

FIGURE 1. Molecular characteristics of the ovarian cancer cell line UWB1.289. **A.** H&E-stained paraffin section of the recurrent tumor from which the UWB1.289 cell line was derived. **B.** DNA extracted from the patient's lymphocytes (germline) and from UWB1.289 cells was sequenced for the BRCA1 mutation 2594delC. The patient's germline DNA was heterozygous for the BRCA1 mutation, whereas the cell line was homozygous. **C.** A protein truncation test (*in vitro* translation) showed heterozygosity of a mutant fragment of BRCA1 exon 11 detected in the patient's germline, but homozygosity in UWB1.289 cells for BRCA1. The wild-type BRCA1 protein fragment (not detected in the UWB1.289 cells) was *in vitro* transcribed from a BRCA1 exon 11 PCR fragment of 3,375 bp. **D.** DNA extracted from UWB1.289 cells was sequenced in all coding exons for the *p53* gene. The p53 mutation 625delAG mutation was found in UWB1.289 cell line DNA but not in the patient's germline DNA (data not shown). **E.** Quantitative reverse transcription-PCR was done using BRCA1 cDNA primers that spanned regions in exons 2 to 7 (primer set 1, *filled columns*) and in exons 9 to 11 (primer set 2, *open columns*). BRCA1 mRNA expression was normalized to endogenous glyceraldehyde-3-phosphate dehydrogenase (*GAPDH*) expression. Columns, mean for two duplicate samples; bars, SE. **F.** Karyotype analysis of the UWB1.289 cell line. Four copies of multiple chromosomes were noted, whereas two copies of chromosome 17 (which contain the *BRCA1* allele) were detected.

developed UWB1.289+BRCA1, a stable cell line in which wild-type BRCA1 function has been restored, as shown by partial rescue of the response to DNA damage. In addition, comparative expression array analysis of the two cell lines revealed BRCA1 involvement in the positive regulation of cell adhesion, invasion, and metastasis-associated genes, including members of the claudin family of genes implicated in cancer invasion and metastasis (21, 22). Array data also revealed a strong association between BRCA1 expression and the down-regulation of multiple IFN-inducible genes. Importantly, the direct propagation of UWB1.289 from an ovarian tumor of papillary serous histology will facilitate further critical analyses of BRCA1 function in ovarian cancer.

Results

Molecular Characterization of the UWB1.289 Ovarian Tumor Cell Line

A germline *BRCA1* mutation 2594delC was identified by the protein truncation test and confirmed by DNA sequencing of lymphocyte DNA from a woman with ovarian cancer. The *BRCA1* mutation 2594delC leads to a stop at codon 845 of *BRCA1*. The 2594delC *BRCA1* mutation has been previously reported in women with familial breast and ovarian cancer.[6] The proband developed breast cancer at age 42, ovarian cancer at age 54, and died at age 56. The proband's mother developed premenopausal breast and then ovarian cancer at age 32 and 40, respectively, and died at age 42. The patient had received no previous radiation. Chemotherapy after optimal cytoreduction consisted of taxol and carboplatinum for six cycles with a complete response, followed by three cycles of taxol on a consolidation trial. Three months after completing chemotherapy, she presented with a symptomatic intra-abdominal recurrence. She received three cycles of topotecan with progressive disease then received gemcitabine and Adriamycin chemotherapy with a partial response. Tumor was collected from a surgery done to bypass a persistent enterovaginal fistula. The interval between chemotherapy and surgery was 1 month. The patient's postoperative course was complicated and consistent with progressive disease. After 6 weeks, she elected hospital discharge with hospice care. She expired 1 week later.

The recurrent ovarian tumor (Fig. 1A) and the cell line derived from the tumor carry the germline *BRCA1* mutation 2594delC (Fig. 1B). Protein truncation tests further showed the lack of a wild-type *BRCA1* coding sequence in the cell line (Fig. 1C). Genotyping of intragenic markers in tumor and cell line DNA confirmed loss of the wild-type *BRCA1* allele (data not shown). A somatic *p53* frameshift mutation in exon 6 (625delAG; Fig. 1D) and loss of the wild-type *p53* allele were detected in tumor and cell line DNA, but not in germline DNA. Sequencing of the entire coding region of phosphatase and tensin homologue deleted on chromosome 10 (*PTEN*) revealed no germline or somatic mutations (data not shown).

Two PCR primer sets were used to amplify BRCA1 message from UWB1.289 cells: primer set 1 (spanning exons 2-7) and primer set 2 (exons 9-11). One-step, real-time reverse transcription-PCR analysis of total RNA revealed expression of mutant BRCA1 transcript in UWB1.289 cells at about half the level of wild-type BRCA1 message when compared with control MCF7 cells (Fig. 1E).

UWB1.289 cells revealed a complex near-tetraploid karyotype that included two copies of chromosome 17 containing the mutant *BRCA1* allele and consistent abnormalities of all chromosomes except chromosome 22 (Fig. 1F). Unstable alterations included dicentric chromosomes, triradials, quadriradials, and double minutes. UWB1.289 cells stained positive for proteins characteristic of the immunophenotype of ovarian carcinoma (cytokeratin 7, calretinin, and Wilms' tumor protein) but negative for the gastrointestinal epithelium marker cytokeratin 20 (data not shown). UWB1.289 cells were estrogen receptor and progesterone receptor negative and did not overexpress HER-2/*neu* as determined by immunohistochemistry (data not shown). Paraffin sections of the patient's primary ovarian tumor as well as the recurrent tumor from which the cell line was derived showed similar staining compared with the UWB1.289 cell line for all proteins investigated (data not shown).

Wild-type BRCA1 Is Expressed in the Stable Cell Line UWB1.289+BRCA1

A pcDNA3 plasmid carrying wild-type *BRCA1* and a hemagglutinin tag (23) was stably transfected into UWB1.289 cells. Nuclear extracts from UWB1.289 cells revealed no wild-type BRCA1 protein expression, whereas UWB1.289+BRCA1 cells showed a high level of wild-type BRCA1 protein expression, comparable with that expressed by control HBL100 mammary epithelial cells (Fig. 2A). Mutant BRCA1 protein expression (predicted to migrate to ~ 93 kDa) in the UWB1.289 cell line could not be discerned from that of alternatively spliced isoforms of BRCA1 (data not shown; refs. 24-27). We confirmed that the wild-type BRCA1 protein observed in UWB1.289+BRCA1 cells was expressed from the stably integrated pcDNA3 plasmid by immunoblotting with an anti-hemagglutinin antibody (Fig. 2B). Growth rates of the UWB1.289 (doubling time = 15.3 h) and UWB1.289+BRCA1 (doubling time = 20.0 h) cell lines were not significantly different.

Because BRCA1 is phosphorylated in response to DNA damage (20, 28, 29), we wished to show that the wild-type BRCA1 protein expressed in UWB1.289+BRCA1 cells was potentially functional in the DNA damage response. We irradiated the mutant and reconstituted cell lines 5 h before

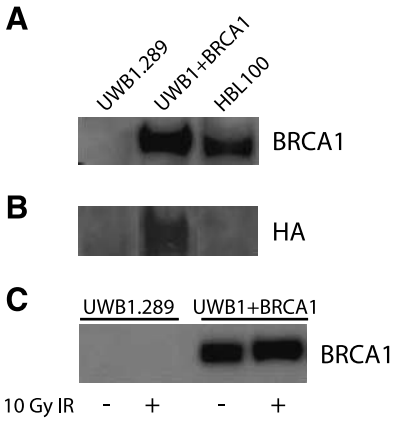

FIGURE 2. Wild-type BRCA1 protein expression in the UWB1.289 and UWB1.289+BRCA1 cell lines. Protein concentration in nuclear protein extracts from UWB1.289, UWB1.289+BRCA1, and HBL100 cells was measured using a colorimetric detergent-compatible Protein Assay (Bio-Rad), and equal amounts of protein were loaded in each lane. **A** and **C.** Western blots were probed with the anti–NH_2-terminal BRCA1 antibody MS110. UWB1.289 cells show no wild-type BRCA1 protein expression. **B.** Western blot was probed with a rat monoclonal anti-hemagglutinin (*HA*) antibody. **C.** Wild-type BRCA1 protein expression was compared in untreated UWB1.289 and UWB1.289+BRCA1 cells and in cells irradiated 5 h before protein extraction. Wild-type BRCA1 expressed by UWB1.289+BRCA1 cells showed a slight mobility shift after irradiation, likely secondary to phosphorylation.

[6] Breast Cancer Information Core mutation database: http://research.nhgri.nih.gov/bic/.

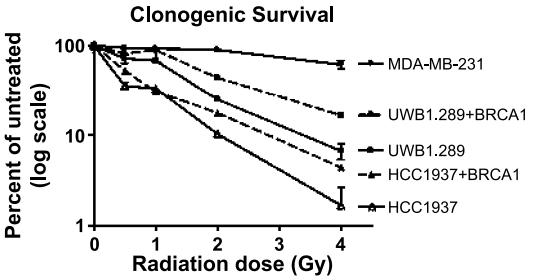

FIGURE 3. UWB1.289 cells are radiation sensitive. Cells were plated in triplicate and irradiated with the indicated dose. After 10 to 14 d, cells were stained with crystal violet and counted visually. Clonogenic survival was calculated as the number of colonies present in each plate normalized to the number of colonies in the unirradiated control plates. Low levels of clonogenic survival indicate sensitivity to IR. Radiation-sensitive UWB1.289 and HCC1937 cells are BRCA1-null and p53 mutant. Nonsensitive MDA-MB-231 cells are BRCA1 wild type and p53 mutant. Points, mean of triplicate samples; bars, SE.

harvesting nuclear protein extracts. Western blot analysis revealed a slight mobility shift in the migration of wild-type BRCA1 protein in response to irradiation in UWB1.289+BRCA1 cells, indicating at least partial phosphorylation of wild-type BRCA1 in response to IR (Fig. 2C).

Wild-type BRCA1 Partially Corrects the Radiation Sensitivity of UWB1.289 Cells

IR induces double-stranded DNA breaks in cellular DNA, and deficiencies in double-stranded DNA break repair are apparent in cells that are sensitive to IR. Impaired colony formation is characteristic of cells following IR exposure. We examined colony formation capacity in the UWB1.289 and UWB1.289+BRCA1 cell lines compared with control MDA MB-231 (BRCA1 wild-type and p53 mutant) and HCC1937 (BRCA1-null and p53 mutant) cancer cell lines. The UWB1.289 cell line showed increased radiation sensitivity (decreased clonogenic survival) with increasing doses of IR (Fig. 3), consistent with the response observed in the HCC1937 cell line. Loss of p53 in tumor cell lines does not induce radiation sensitivity, illustrated by the response of MDA MB-231 cells to IR. UWB1.289+BRCA1 cells showed a partial correction of radiation sensitivity, evidenced by increased clonogenic survival at higher IR doses. This response was similar to, but relatively greater than, the gain of function observed in HCC1937+BRCA1 cells.

BRCA1 Contributes to S-Phase Arrest in UWB1.289 Cells after IR-Induced DNA Damage

To repair damaged DNA, cells use DNA damage checkpoints to slow down or halt DNA replication (S phase) and progression to mitosis (M phase; ref. 30). Although p53 is important in the G_1-S phase checkpoint (31), BRCA1 has been implicated in both the S and G_2-M phase DNA damage checkpoints (32, 33). To determine the effect of BRCA1 on cell cycle checkpoints in UWB1.289 cells, we examined cell cycle distribution following DNA damage induced by IR in UWB1.289 and UWB1.289+BRCA1 cells. Fifteen and 24 h after IR, UWB1.289 cells show a decrease in the percentage of cells in G_1, consistent with other cells that have acquired mutations in *p53* (Fig. 4A). UWB1.289 cells also show a lack of S-phase arrest, suggesting a loss of capacity to slow DNA replication in the presence of IR-induced DNA damage. This cell cycle distribution phenotype is consistent with that observed in HCC1937 cells.

Restoration of BRCA1 function in the UWB1 cell line results in an increase in the percentage of cells in S phase 15 h after IR, suggesting that wild-type BRCA1 functions to arrest cells in S-phase arrest and prevent them from entering G_2-M phase in the presence of DNA damage. We further evaluated the role of BRCA1 in S-phase arrest by examining radioresistant DNA synthesis in UWB1.289 and UWB1.289+BRCA1 cells. Radioresistant DNA synthesis occurs when DNA synthesis continues in the presence of DNA damage, indicating a compromised S-phase checkpoint (34). Fifteen hours after IR, UWB1.289+BRCA1 cells showed a partial correction of

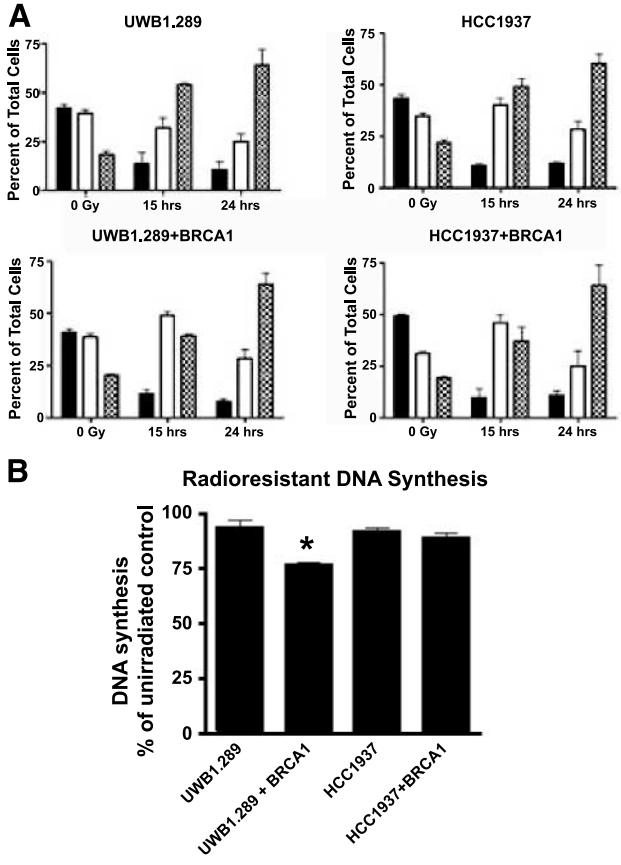

FIGURE 4. Cell cycle distribution and radioresistant DNA synthesis are compromised in UWB1.289 cells but restored in UWB1.289+BRCA1 cells. **A.** Logarithmically growing cells were irradiated with 10 Gy IR and incubated for either 15 or 24 h. Cells were harvested and analyzed by flow cytometry. Black columns, cells in G_1 phase; open columns, cells in S phase; checkered columns, cells in G_2-M phase. Columns, mean of two to five replicate experiments; bars, SE. UWB1.289+BRCA1 cells show an increase in the percentage of cells in S phase 15 h after irradiation. **B.** Logarithmically growing cells were plated in triplicate, and DNA synthesis was measured 15 h after IR as described in Materials and Methods. Decreased DNA synthesis in UWB1.289+BRCA1 cells shows functional slowing of DNA replication after IR-induced DNA damage. *, $P < 0.001$, significant difference in DNA synthesis between UWB1.289 and UWB1.289+BRCA1 cells.

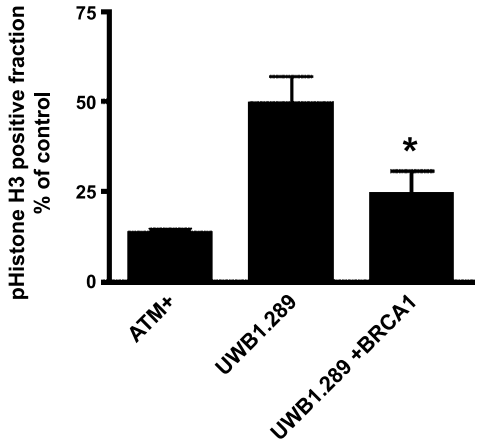

FIGURE 5. BRCA1 partially restores the G_2-M DNA damage checkpoint. Cells were irradiated with 6 Gy IR, and mitotic cells (phosphorylated histone H3–positive fraction) were calculated as a percentage of the mitotic cells present in the unirradiated control sample 24 h after IR. Cells with a functional G_2-M checkpoint (the ATM-positive cell line) maintain a greater percentage of cells in G_2 phase in the presence of DNA damage, and the fraction that stains positive for phosphorylated histone H3 is small. UWB1.289 cells reveal a compromised G_2-M DNA damage checkpoint, but BRCA1 partially restores this function in UWB1.289+BRCA1 cells.

the S-phase checkpoint defect noted in UWB1.289 cells, as illustrated by a significant decrease in DNA synthesis (Fig. 4B). This corrective effect was more pronounced in UWB1.289+BRCA1 cells than in HCC1937+BRCA1 cells.

BRCA1 Functions to Restore G_2-M Arrest in UWB1.289+BRCA1 Cells

The G_2-M DNA damage checkpoint arrests cells in G_2, preventing cell division and transmission of damaged DNA to daughter cells. Because the amount of DNA in both G_2 and M phase cells is 4n, the cell cycle distribution assay (which shows accumulation of UWB1.289 cells in G_2-M phase by measuring cellular DNA content; see Fig. 4A) cannot distinguish between cells arrested in G_2 and those allowed entry into M phase. We therefore used a mitotic cell marker, phosphorylated histone H3, in a checkpoint assay to delineate G_2 versus M phase cells (32, 35). In comparison with ATM-positive control cells, which have a functional G_2-M checkpoint (32, 36), UWB1.289 cells seem to have lost this critical DNA damage checkpoint. This is illustrated by a high percentage of mitotic cells, versus cells arrested in G_2, that accumulate after IR-induced DNA damage in UWB1.289 cells (Fig. 5). Consistent with previous reports that ascribe a role for BRCA1 function in the G_2-M phase DNA damage checkpoint, we observed a significant reduction in the percentage of mitotic cells after exposure to IR in UWB1.289+BRCA1 cells.

BRCA1 Negatively Regulates Expression of IFN-Inducible Genes

We next sought to define how gene expression is altered after IR exposure when wild-type BRCA1 is restored to a BRCA1-null ovarian cancer cell line. We did gene expression array experiments to examine the effect of wild-type BRCA1 expression in UWB1.289 cells following IR-induced DNA damage. Table 1 lists genes both up- and down-regulated at least 3-fold in UWB1.289+BRCA1 cells compared with UWB1.289 cells, 5 h after IR-induced DNA damage. Consistent with our protein expression data, wild-type BRCA1 expression was almost 9-fold higher in UWB1.289+BRCA1 cells compared with UWB1.289 cells ($P < 0.005$). When a P cutoff level of <0.0005 was used in the analysis, 28 genes were found to be up-regulated, whereas 23 genes were observed to be down-regulated at least 3-fold in UWB1.289+BRCA1 cells compared with UWB1.289 cells after IR-induced DNA damage. If $P < 0.001$ was used with a threshold fold change of 2.0, then 95 genes were up-regulated, and 89 genes were down-regulated (data not shown). Ontology analysis (fold change threshold = 2.0, $P < 0.005$) showed that multiple cell adhesion genes were up-regulated (z score = 2.8), whereas genes involved in the immune response were down-regulated (z score = 5.9; data not shown).

Because we observed partial restoration of DNA repair and cell cycle checkpoint function in UWB1.289+BRCA1 cells after IR, and because BRCA1 associates directly with multiple proteins involved in DNA repair and cell cycle checkpoint regulation (9, 10), we hypothesized that some of these genes would be up-regulated in UWB1.289+BRCA1 cells compared with UWB1.289 cells after IR. Of the BRCA1-associated genome surveillance protein complex proteins described to date (37), MRE11 was up-regulated 1.3-fold ($P = 0.001$), RAD50 was up-regulated 1.6-fold ($P = 0.01$), and MSH6 was up-regulated 1.4-fold ($P = 0.04$). Expression of ATM, ATR, NBS1, MLH1, and MSH2 was not significantly altered. The double-strand break repair gene *RAD51* (1.6-fold, $P = 0.004$) and the Bloom syndrome gene *BLM* (1.3-fold, $P = 0.04763$) were both down-regulated in UWB1.289+BRCA1 versus UWB1.289 cells in response to IR.

We also observed significant down-regulation of multiple IFN-inducible (IFI) genes in UWB1.289+BRCA1 cells after IR (see Table 1). Of the 23 down-regulated genes listed in Table 1, the four genes that showed the greatest fold-change in expression were *IFI16* (17×), *IFI44* (10×), *IFI27* (8×), and *IFITM1* (6×). In addition, MX1 (IFN-inducible protein p78) was down-regulated 4-fold in UWB1.289+BRCA1 cells following IR. This effect was not due to irradiation, as microarray analyses of nonirradiated UWB1.289 and UWB1.289+BRCA1 cells also revealed down-regulation of IFN-responsive genes in UWB1.289+BRCA1 cells (Table 2). Also listed in Table 2 are expression data for a selected set of genes identified as significant in our analysis in both irradiated and untreated cells.

Discussion

We propagated a new human, ovarian BRCA1-null cell line (UWB1.289) from a recurrent tumor of a patient with ovarian cancer. The patient's clinical course was consistent with primary platinum refractory disease according to standard definitions of platinum sensitivity in patients with ovarian cancer, and her overall survival was only 24 months. Women with *BRCA1*-associated ovarian cancers are generally thought to have a better survival than those with sporadic ovarian cancer, and BRCA1-deficient tumors generally display increased sensitivity to platinum chemotherapy *in vitro* (38-43). It has been difficult to generate cell lines from BRCA1-associated

Table 1. Genes Up-Regulated and Down-Regulated at Least 3-fold in Irradiated UWB1.289+BRCA1 Cells Compared to Irradiated UWB1.289 Cells ($P < 0.0005$)

Gene ID	Gene name	Gene identifier	Fold change	*P*
Genes up-regulated				
BRCA1	Breast cancer 1, early onset	AF005068	8.8	0.0018
CLDN6	Claudin 6	NM_021195	15.3	0.000010
MGC33926	Hypothetical protein MGC33926	AA058832	13.5	0.000003
EDIL3	EGF-like repeats and discoidin I-like domains 3	AA053711	12.9	0.000061
NPR3	Natriuretic peptide receptor C/guanylate cyclase C (atrionatriuretic peptide receptor C)	NM_000908	10.8	0.000214
TIMP3	TIMP metallopeptidase inhibitor 3 (Sorsby fundus dystrophy, pseudoinflammatory)	BF347089	10.3	0.000142
NID2	Nidogen 2 (osteonidogen)	NM_007361	8.9	0.000026
FLJ14054	Hypothetical protein FLJ14054	NM_024563	8.5	0.000072
PTGER2	Prostaglandin E receptor 2 (subtype EP2), 53 kDa	NM_000956	8.5	0.000042
TIMP3	TIMP metallopeptidase inhibitor 3 (Sorsby fundus dystrophy, pseudoinflammatory)	NM_000362	8.2	0.000079
CLDN6	Claudin 6	AW003929	6.9	0.000424
VGLL1	Vestigial like 1 (*Drosophila*)	BE542323	6.9	0.000011
VGLL1	Vestigial like 1 (*Drosophila*)	NM_016267	6.1	0.000256
—		BF344237	5.6	0.000164
CDH6	Cadherin 6, type 2, K-cadherin (fetal kidney)	BC000019	5.3	0.000125
CDH6	Cadherin 6, type 2, K-cadherin (fetal kidney)	NM_004932	5.2	0.000157
CDH6	Cadherin 6, type 2, K-cadherin (fetal kidney)	BC000019	4.8	0.000401
ZNF365	Zinc finger protein 365	NM_014951	4.6	0.000042
GNAQ	Guanine nucleotide binding protein (G protein), q polypeptide	AA628423	4.4	0.000065
LRRN1	Leucine-rich repeat neuronal 1	N71874	4.4	0.000069
—	*Homo sapiens*, clone IMAGE:4710650, mRNA	BF696216	4.2	0.000293
ARID5B	AT rich interactive domain 5B (MRF1-like)	BG285011	4.1	0.000370
CCL2	Chemokine (C-C motif) ligand 2	S69738	4.1	0.000248
GNAQ	Guanine nucleotide binding protein (G protein), q polypeptide	BF969428	4.0	0.000042
SFRP1	Secreted frizzled-related protein 1	AF017987	4.0	0.000023
FZD7	Frizzled homologue 7 (*Drosophila*)	NM_003507	4.0	0.000288
C12orf46	Chromosome 12 open reading frame 46	AI051248	3.9	0.000009
KIAA1505	Postmeiotic segregation increased 2-like 11	AB040938	3.8	0.000031
POU3F3	POU domain, class 3, transcription factor 3	AW149422	3.6	0.000014
SFRP1	Secreted frizzled-related protein 1	AF017987	3.6	0.000340
DENND2A	DENN/MADD domain containing 2A	AA127623	3.5	0.000351
DKFZP686A01247	DKFZP686A01247 hypothetical protein	AK026815	3.4	0.000240
TIMP3	TIMP metallopeptidase inhibitor 3 (Sorsby fundus dystrophy, pseudoinflammatory)	U67195	3.4	0.000097
GNAQ	Guanine nucleotide binding protein (G protein), q polypeptide	BF222895	3.3	0.000214
OXTR	Oxytocin receptor	NM_000916	3.3	0.000262
GFBP5	Insulin-like growth factor binding protein 5	AW007532	3.2	0.000106
TPK1	Thiamin pyrophosphokinase 1	AB028138	3.1	0.000011
Genes down-regulated				
IFI16	INF, γ-inducible protein 16	AF208043	17.0	0.000248
IFI16	IFN, γ-inducible protein 16	NM_005531	16.9	0.000082
IFI44	IFN-induced protein 44	NM_006417	9.7	0.000162
IFI27	IFN, α-inducible protein 27	NM_005532	8.3	0.000012
IFITM1	IFN-induced transmembrane protein 1 (9-27)	AA749101	6.3	0.000264
HHEX	Homeobox, hematopoietically expressed	Z21533	5.6	0.000007
LOC151760	Hypothetical LOC151760	BC038577	5.1	0.000288
PDZK1IP1	PDZK1 interacting protein 1	NM_005764	5.0	0.000001
AOX1	Aldehyde oxidase 1	NM_001159	4.7	0.000011
SUNC1	Sad1 and UNC84 domain containing 1	AI221329	4.4	0.000008
LCP1	Lymphocyte cytosolic protein 1 (L-plastin)	J02923	4.2	0.000105
PDZK1IP1	PDZK1 interacting protein 1	NM_005764	4.0	0.000190
—		AL031290	4.0	0.000050
MX1	Myxovirus (influenza virus) resistance 1, IFN-inducible protein p78 (mouse)	NM_002462	3.7	0.000174
CDC42EP5	CDC42 effector protein (Rho GTPase binding) 5	AW084544	3.7	0.000062
ECM2	Extracellular matrix protein 2, female organ and adipocyte specific	NM_001393	3.7	0.000289
LRRC34	Leucine-rich repeat containing 34	AW975772	3.6	0.000003
PROCR	Protein C receptor, endothelial (EPCR)	NM_006404	3.5	0.000338
LRRC34	Leucine-rich repeat containing 34	AW975772	3.5	0.000401
MYLK	Myosin, light polypeptide kinase	AA526844	3.4	0.000320
ATG3	ATG3 autophagy related 3 homologue (*Saccharhomyces cerevisiae*)	NM_022488	3.4	0.000476
ADAMTS9	ADAM metallopeptidase with thrombospondin type 1 motif, 9	AL832835	3.3	0.000307
—		AA470369	3.2	0.000035
PMCH	Pro-melanin-concentrating hormone	AI224977	3.2	0.000070
VARSL	Valyl-tRNA synthetase like	BE222664	3.2	0.000087
SLC43A3	Solute carrier family 43, member 3	AI630178	3.1	0.000182

NOTE: All cells were treated with 10 Gy IR 5 h before RNA extraction.

ovarian cancers. It is interesting to speculate that the molecular features that contributed to this patient's unusually aggressive clinical course may also have facilitated propagation of the tumor *in vitro*.

We characterized the UWB1.289 cell line's molecular features and also studied its function relative to the DNA damage response. Consistent with previous reports for the BRCA1-null breast cancer cell line HCC1937, the

Table 2. Selected Genes of Interest from Oligonucleotide Array-Based Expression Profiling of UWB1.289+BRCA1 Compared with UWB1.289 Cells

Gene ID	Gene name	Direction	Gene identifier	Fold change +IR	*P*	Fold change untreated	*P*
IFN-inducible genes							
IFI16	IFN, γ-inducible protein 16	Down	AF208043	17.0	0.00025	23.7	0.00006
IFI27	IFN, α-inducible protein 27	Down	NM_005532	8.3	0.00001	7.9	0.04150
IFITM1	IFN-induced transmembrane protein 1 (9-27)	Down	AA749101	6.3	0.00026	4.4	0.04423
IFI44	IFN-induced protein 44	Down	NM_006417	9.7	0.00016	5.6	0.01245
IFI35	IFN-induced protein 35	Down	BC001356	5.6	0.00329	2.7	0.03976
IFIT3	IFN-induced protein with tetratricopeptide repeats 3	Down	AI075407	3.3	0.00070	2.6	0.01928
ISG20	IFN-stimulated exonuclease gene 20 kDa	Down	U88964	1.9	0.00426	2.0	0.04224
IFITM3	IFN-induced transmembrane protein 3 (1-8U)	Down	BF338947	1.8	0.00033	2.1	0.00336
IFITM2	IFN-induced transmembrane protein 2 (1-8D)	Down	NM_006435	1.7	0.00849	2.2	0.00830
Genes associated with cell adhesion, invasion, and metastasis							
CLDN6	Claudin 6	Up	AW003929	6.9	0.00042	9.8	0.02518
CLDN11	Claudin 11 (oligodendrocyte transmembrane protein)	Down	AW264204	5.3	0.00055	4.1	0.00395
CDH6	Cadherin 6, type 2, K-cadherin (fetal kidney)	Up	NM_004932	6.2	0.00057	3.6	0.01399
EDIL3	EGF-like repeats and discoidin I-like domains 3	Up	AA053711	12.9	0.00006	9.4	0.00476
FLRT2	Fibronectin leucine-rich transmembrane protein 2	Up	NM_013231	2.1	0.00365	4.3	0.04404
NID2	Nidogen 2 (osteonidogen)	Up	NM_007361	8.9	0.00003	6.5	0.01368
RASA1	RAS p21 protein activator (GTPase activating protein) 1	Up	M23612	2.1	0.00498	1.4	0.00375
COL8A1	Collagen, type VIII, α 1	Down	BE877796	2.1	0.00046	2.4	0.03302
ECM2	Extracellular matrix protein 2, female organ and adipocyte specific	Down	NM_001393	3.7	0.00029	4.9	0.00162

NOTE: Data are presented as genes up-regulated or down-regulated in UWB1.289+BRCA1 cells compared with UWB1.289 cells under the same condition (+IR or untreated).

UWB1.289 cell line is deficient in DNA repair and cell cycle checkpoint function. Stable transfection of wild-type *BRCA1* into the UWB1.289 cell line (UWB1.289+BRCA1) showed partial correction of DNA repair defects and cell cycle checkpoint function in response to IR-induced DNA damage. In addition, results of expression array experiments reveal a novel function for BRCA1 in the positive regulation of selected set of cell adhesion, invasion, and metastasis-related genes and the negative regulation of multiple IFN-inducible genes.

The SNU251 cell line is the only ovarian cancer BRCA1-null cell line that has been examined relative to BRCA1 function in the DNA damage response (14). SNU251 is of endometrioid histology and thus represents a less common histologic type (~ 15%) of ovarian cancer (44). SNU251 carries a heterozygous missense mutation in MLH1, and it is unknown if the BRCA1 mutation in SNU-251 originated in the patient's germline or as a somatic mutation in the tumor or cell line (14). SNU251 has a nonsense mutation (5564G>A) in exon 23 of *BRCA1,* resulting in mutant BRCA1 protein that is truncated at the COOH terminus by only 48 amino acids yet is expressed at a high level in the mutant cell line (14).

Very recently, two ovarian cancer BRCA1-null cell lines (PD-OVCA1 and PD-OVCA2) were reported that, similar to UWB1.289, represent papillary serous cancer, the most common histologic subtype of ovarian cancer (15). These two lines were developed from tumor xenografts and were characterized genetically and histologically but not functionally. Interestingly, PD-OVCA1 revealed multiple mutant *BRCA1* alleles, similar to our finding that chromosome 17 is duplicated in the UWB1.289 cell line. It is unclear if the amplification of the chromosome containing the mutant *BRCA1* allele contributes to expedited ovarian tumorigenesis, as others have observed this genetic phenomena in breast tumors (45). Thus, studies designed using both the PD-OVCA1 and UWB1.289 cell lines have the potential to reveal a role for BRCA1 in the most common type of ovarian cancer.

The HCC1937 cell line is the only BRCA1-null cell line in which the DNA damage response to IR has been extensively studied (46). This cell line carries a *BRCA1* mutation in exon 20 (5382insC), resulting in the loss of 34 amino acids from the COOH terminus. Although the *BRCA1* mutation in HCC1937 cells is in the COOH terminus (versus exon 11 in UWB1.289 cells), many molecular characteristics of the two cell lines (estrogen receptor and progesterone receptor status, *p53* mutation, and ploidy) are similar, as well as the impaired response to IR-induced DNA damage, as revealed in this study. Yet, homozygous deletion of *PTEN* in HCC1937 cells (46) could complicate evaluation of the role of BRCA1 in the DNA damage response in this cell line. UWB1.289 has no discernible defect in *PTEN,* providing a complementary cell line for analyses of BRCA1 function. Initial studies concluded that HCC1937 cells were sensitive to IR and deficient in double-strand break repair (20, 23, 47) but retained normal S-phase and G_2-M cell cycle checkpoints (23). In contrast, subsequent studies of HCC1937 cells showed defective G_2-M and S-phase cell cycle checkpoints in response to IR (32, 48). Additional conflicting results from HCC1937 cells were reported recently with respect to G_2-M checkpoint function (49, 50) and nonhomologous end-joining of double-strand break repair (29, 51-53), suggesting that additional experimental systems are necessary to thoroughly delineate the function of BRCA1 in the DNA damage response.

In expression array experiments that compared gene expression following exposure to IR between UWB1.289+BRCA1 and UWB1.289 cells, we found that although DNA repair and cell cycle checkpoint genes were generally up-regulated in UWB1.289+BRCA1 cells compared with

UWB1.289 cells, the effect was modest. This finding is consistent with the results of our functional assays that showed only a partial (but in most experiments, significant) correction of deficiencies in the DNA damage response in UWB1.289+ BRCA1 cells.

In our expression array experiments, more pronounced gene expression alterations were found in extracellular matrix and IFN-regulated genes. We observed significant up-regulation of claudin 6 and down-regulation of claudin 11 in UWB1.289+BRCA1 cells compared with UWB1.289 cells, both in untreated cells and those exposed to irradiation. Because regulation of the claudin genes is not due to irradiation in this study, it is likely the result of expression of wild-type BRCA1 in UWB1.289 cells. To our knowledge, a link between claudins and BRCA1, or between claudin 11 and cancer, has not been shown previously. Claudin genes, which code for tight junction proteins, are believed to play a role in cancer cell invasion and metastasis (21, 22) and have been implicated in breast and ovarian cancer. Reduced expression of claudin 7 was associated with invasion and metastasis of esophageal cancers (54). Claudin 3 was recently shown to be down-regulated in invasive, compared with noninvasive, breast cancer cells (55). Interestingly, claudin 6 expression, which we found to be highly up-regulated in the presence of wild-type BRCA1, was preferentially expressed in mammary epithelial cells from Copenhagen rats, which are resistant to mammary cancer, versus more susceptible Buffalo rats (56). The same authors found reduced expression of claudin 6 in human breast cancer cell lines and tissue samples in comparison with normal breast tissue. Our observations are intriguing in that they suggest a role for BRCA1 in the maintenance of claudin 6 expression and thus the metastatic potential of ovarian cancer.

In addition to the claudin genes, our expression array experiments revealed BRCA1 regulation of multiple additional genes associated with cell adhesion processes. Strikingly, many of these genes encode extracellular matrix proteins (*CLDN6, CLDN11, CDH6, FLRT2, COL8A1*, and *ECM2*) that function as cell-cell adhesion molecules. These genes normally play a key role in cell morphogenesis and maintenance of orderly structure and, when disrupted, may contribute to the invasion and metastasis of cancer. Interestingly, a previous study found that reverse transcription-PCR detected FLRT2 expression in a number of human tissues, with highest expression in the ovary (57).

IFN-responsive genes have been identified previously in gene expression array experiments in relation to BRCA1. Andrews et al. observed that multiple IFN-inducible genes were up-regulated in response to up-regulated BRCA1 expression in a tetracycline-regulated breast cancer cell line (58). These studies were only done in duplicate; therefore, significance levels were unknown. In contrast, Jazaeri et al. identified a set IFN-responsive genes that were up-regulated in ovarian tumors, including BRCA1-mutated tumors versus SV40-immortalized ovarian surface epithelial cell lines (59). In both our analysis and the Jazaeri et al. experiments, IFN-inducible transmembrane protein 1 (9-27) was down-regulated in the samples with wild-type BRCA1, suggesting a role of BRCA1 in disruption of the IFN-inducible pathway in a subset of ovarian cancers. Interestingly, a recent study found that overexpression of IFN-inducible 9-27 in gastric cancer cells was associated with increased resistance to immune cells and invasive potential (60).

IFI16, a member of the IFN-inducible p200 protein family, was down-regulated in irradiated (17-fold) and untreated (24-fold) UWB1.289+BRCA1 cells compared with UWB1.289 cells under the same conditions (see Table 2). *IFI16* is one of the few IFN-inducible genes directly involved in the regulation of cell proliferation and differentiation (61). There is increasing evidence that members of the IFI p200 family (including *IFI16*) may be regulated by stimuli, independent of the IFNs (59, 61, 62). In our array analysis, we observed down-regulation of multiple IFN-inducible genes when wild-type BRCA1 was expressed. Strikingly, down-regulation of these genes occurred in the absence of any measured changes in expression of IFN genes, such as *IFN-α* or *IFN-γ*. Thus, our study suggests that BRCA1-mediated regulation of IFN-inducible genes may be one alternate mechanism of IFN-inducible gene activation.

In summary, we describe the molecular features of a novel BRCA1-null ovarian cancer cell line UWB1.289 and examine the role of BRCA1 in the DNA damage response in this cell line in comparison with UWB1.289 cells in which wild-type BRCA1 expression has been stably reconstituted. UWB1.289 cells are sensitive to radiation and lack both S and G_2-M cell cycle checkpoints. Restoration of wild-type BRCA1 expression in UWB1.289 cells partially corrects these DNA damage response deficits. This result is supported by increased expression of DNA repair and cell cycle genes in response to IR in UWB1.289+BRCA1 cells. In addition, our expression array experiments revealed that expression of a set of extracellular matrix genes was notably altered, whereas a set of IFN-inducible genes were significantly down-regulated, in cells not as a result of exposure to IR but as a result of restoration of wild-type BRCA1 expression in UWB1.289 cells. Because these genes are known to play a role in cell invasion and metastasis and seem to be regulated by BRCA1, we suspect that they are involved in ovarian carcinogenesis. Finally, because the vast majority of reports of BRCA1 function have been based solely on studies done in breast cancer cell line HCC1937 (20, 23, 32, 47, 50), we expect that experiments in additional BRCA1-null cell lines will enable more robust conclusions regarding BRCA1 function, particularly the elucidation of the role of BRCA1 in ovarian tumorigenesis.

Materials and Methods

Tissue Culture and Irradiation Treatment

The HBL-100 and MDA MB 231 cell lines were purchased from the American Type Culture Collection (Manassas, VA) and maintained as directed. The HCC1937 cell line was a generous gift from Dr. Gail Tomlinson (University of Texas Southwestern Medical Center), and HCC1937+BRCA1 cells were developed in Dr. Weixin Wang's laboratory with a protocol identical to that used to reconstitute wild-type BRCA1 in the UWB1.289 cell line (see below). The AT221JETpEBS7-YZ5 (ATM positive) cell line was a generous gift from Dr. Yosef Shiloh (Tel Aviv University, Israel) and was maintained as described (63). The UWB1.289 cell line was maintained in 50%

RPMI + 50% MEGM, supplemented with 3% fetal bovine serum, and UWB1.289+BRCA1 was maintained in the same media plus 200 μg/mL G418. The vector pcDNA3-BRCA1 plasmid (23) was generously provided by Dr. David Livingston (Dana-Farber Cancer Institute, Boston, MA) to Dr. Weixin Wang and was transfected into the UWB1.289 cell line using 5 μg Fugene 6 (Roche, Indianapolis, IN) per 100-mm plate of cells, according to the manufacturer's recommendations. Stable cell lines were established by selection of positive clones that grew in media containing G418. Irradiation of cells for DNA damage experiments was done at room temperature using a Gammacell 40 ^{137}Cesium irradiator (Atomic Energy of Canada, Ltd., Mississauga, Ontario, Canada). All flow cytometry was done in the flow cytometry core facility of Dr. Peter Rabinovitch (University of Washington Department of Pathology).

Derivation of UWB1.289

Under approval from the Human Subjects Division of the University of Washington Institutional Review Board, tissue and blood were collected from a patient with a germline *BRCA1* mutation (2594delC) undergoing surgery for recurrent ovarian cancer. Fresh tumor was mechanically minced and plated in several types of media. Pure epithelial clones were isolated by subcloning and differential trypsinization until fibroblasts were eliminated. The tumor cell line was maintained at 37°C with 5% CO_2 in 50% RPMI + 50% MEGM, supplemented with 3% fetal bovine serum. The stable cell line was named UWB1.289 (University of Washington-BRCA1-family 289). Immunohistochemistry was done on cultured cells using cytokeratin AE1/AE3 antibodies to assess epithelial purity.

Molecular Characterization of UWB1.289

The BRCA1 mutation was originally detected by protein truncation tests done on both germline and cell line DNA using PCR amplification of *BRCA1* exon 11 followed by *in vitro* transcription/translation with the TNT T7 Quick for PCR DNA kit (Promega, Madison, WI) and visualization with SDS-PAGE. DNA from lymphocytes and the UWB1.289 cell line were sequenced around *BRCA1* nucleotide 2594 using Big Dye Terminator chemistry and an automated 3100 DNA sequencer (Applied Biosystems, Foster City, CA). Direct DNA sequencing for UWB1.289 was done for all coding exons and flanking regulatory regions of the tumor suppressor genes *TP53* and *PTEN*. Loss of heterozygosity was evaluated at the intragenic *BRCA1* marker D17S855 using standard methodology. Karyotype analysis was done by the University of Washington Cytogenetics core facility on metaphase spreads for five cells of the stable cell line.

One-step real-time reverse transcription-PCR was used to evaluate BRCA1 transcript in total RNA samples extracted from BRCA1-null cell lines with Trizol (Invitrogen, San Diego, CA). A Lightcycler-RNA Amplification kit SYBR Green I (Roche) apparatus was used to evaluate transcript expression (64). A fluorescent dye that binds double-stranded DNA and a real-time fluorescence detection system allow the number of cycles to be calibrated for each amplicon, and cDNA copy numbers are estimated based on an internal standard curve. Two different pairs of BRCA1 primers were used: BRCA1 primer set 1 amplified a region across exons 2 to 7 (forward, 5′-CAAGGAACCTGTCTCCACAAAGTG-3′) and BRCA1 primer set 2 amplified a region across exons 9 to 11 (forward, 5′-CCAACTCTCTAACCTTGGAACTGTG-3′). Glyceraldehyde-3-phosphate dehydrogenase transcript was also amplified and used to normalize the quantity of BRCA1 transcript in each cell line. All reactions were run in duplicate.

Protein Expression Analysis

BRCA1 and hemagglutinin protein expression in cell lines was visualized by SDS-PAGE/Western blot. Nuclear protein extracts were harvested as described (65) during logarithmic cell growth from UWB1.289, UWB1.289+BRCA1, and HBL-100 cells. Protein was quantitated with a colorimetric assay (Bio-Rad, Richmond, CA), and equal amounts of nuclear protein extract were loaded on a Nu-Page 3-8% Tris-Acetate gel (Invitrogen). Proteins were transferred for 4 h to Immun-Blot polyvinylidene difluoride membrane (Bio-Rad). Western blots were blocked for one hour in PBS + 6% nonfat dry milk and probed overnight at 4°C with BRCA1 Ab-1 (MS110; Oncogene Research Products, San Diego, CA) diluted 1:250 in PBS + 0.05% Tween + 3% nonfat dry milk. Blots were washed and probed for 1 h (for BRCA1 visualization) at room temperature with goat anti-mouse horseradish peroxidase–conjugated secondary antibody (Santa Cruz Biotechnology, Santa Cruz, CA) diluted 1:20,000. For hemagglutinin visualization, the blot was stripped and reprobed with a high-affinity rat monoclonal anti-hemagglutinin antibody (Roche) diluted 1:1,000, washed, and then probed with a donkey anti-rat horseradish peroxidase–conjugated secondary antibody (The Jackson Laboratory, Bar Harbor, ME) diluted 1:10,000. Blots were developed using enhanced chemiluminescence (Amersham, Arlington Heights, IL).

Clonogenic Survival

Radiation sensitivity of cell lines was evaluated using methods described previously (23). Cells were plated in triplicate for optimal density at counting. During the logarithmic growth phase, cells were trypsinized and irradiated with 0, 0.5, 1, 2, or 4 Gy IR. After IR, cells were re-plated and incubated in normal culture conditions for 10 to 14 days. Cells were fixed and stained with crystal violet, and colonies having >20 cells were counted visually. The number of colonies counted in each test plate was normalized to the number of colonies counted in unirradiated control plates.

Cell Cycle Distribution

Cells were irradiated during logarithmic growth with 0 or 10 Gy IR. After IR, cells were incubated for 15 or 24 h and then harvested and fixed/labeled with 4′,6-diamidino-2-phenylindole fix solution [10 μg/mL 4′,6-diamidino-2-phenylindole and 0.1% NP40 detergent in TBS (pH 7.4)]. DNA content quantitation and cell cycle analysis were done as previously described (66). Briefly, the cell suspension was triturated with a 26-gauge needle and analyzed using a high-speed Influx flow cytometer and Spigot software (Cytopeia, Inc., Seattle, WA) with UV excitation and 4′,6-diamidino-2-phenylindole emission collected with a 450-40 UV filter. Cell cycle data were analyzed using WinCycle software (Phoenix Flow Systems, San Diego, CA).

Radioresistant DNA Synthesis

Radioresistant DNA synthesis assays were done using protocols modified from previous reports (32, 67). Briefly, 5×10^4 cells were plated in triplicate for 24 h. The culture medium was changed to thymidine-free RPMI + 10% fetal bovine serum + 20 mmol/L HEPES; ^{14}C-thymidine was added to each plate; and the cells were incubated for 15 to 17 h under standard conditions. The ^{14}C-thymidine–containing media was removed; fresh RPMI and HEPES were added; and the cells were irradiated with 0 or 10 Gy IR. Immediately after IR, ^{3}H-thymidine was added to each plate, and the cells were incubated for 15 h. The cells were then washed with PBS and incubated in fresh RPMI for 30 min. After washing, the cells were lysed in 500 μL of 0.25 mol/L NaOH, and the mixed cell suspension was added to 7.5 mL Opti-Fluor scintillation fluid (Packard Bioscience, Meriden, CT). ^{3}H/^{14}C dpm ratios were counted using a dual-label counting program on a Tri-Carb 2300TR liquid scintillation analyzer (Packard Bioscience). DNA synthesis values were calculated as a percentage of the values obtained from unirradiated control cells run in parallel.

G_2-M Checkpoint Analysis

Cells were prepared for G_2-M assays as described previously (32, 50). Briefly, logarithmically growing cells were irradiated with 0 or 6 Gy IR, incubated for 3 h, and treated with 1 μg/mL Nocodazole (Sigma, St. Louis, MO) for 20 h (50). After incubation, cells were trypsinized, harvested, and fixed in 70% ethanol at −20°C for 12 to 48 h. After two washes with PBS, the cells were incubated in 0.25% Triton X-100 on ice for 15 min. Cells were then centrifuged and resuspended in 0.75 μg of rabbit polyclonal, anti–phospho-histone H3 antibody (Upstate Biotechnology, Lake Placid, NY) in 100 μL PBS + 1% bovine serum albumin for 3 h at room temperature. Cells were rinsed with PBS + 1% bovine serum albumin and incubated in Alexa 488–conjugated goat ant-rabbit IgG (The Jackson Laboratory) diluted 1:30 in PBS + 1% bovine serum albumin for 30 min in the dark. Cells were washed with PBS and fixed in 4′,6-diamidino-2-phenylindole fix solution. Flow cytometry analysis was done on the Influx flow cytometer using a 488-nm argon excitation laser and a 525-30 filter to collect Alexa 488 emission. WinCycle software was used for data analysis.

Data Analyses of Functional In vitro *Experiments*

GraphPad Prism software (San Diego, CA) was used to calculate SE and statistical differences with one-way ANOVA analysis and Tukey's multiple comparison post-test using a confidence interval of 95%.

Gene Expression Arrays

Total RNA was extracted from triplicate plates of 10^6 UWB1.289 and UWB1.289+BRCA1 cells 5 h after exposure to 10 Gy IR with Trizol (Sigma) and chloroform. Triplicate plates of 10^6 untreated UWB1.289 and UWB1.289+BRCA1 cells were used to control for the effects of ionizing radiation. RNA was cleaned up using RNEasy midi-columns (Qiagen, Chatsworth, CA), and quality was assessed with a Bioanalyzer 2100. Three RNA samples each from IR-treated and untreated UWB1.289 and UWB1.289+BRCA1 cells (for a total of 12 samples hybridized to 12 chips) were labeled and hybridized to GeneChip Human Genome U133 Plus 2.0 Affymetrix chips at the University of Washington Center for Expression Arrays. Chips were washed and scanned at the University of Washington Center for Expression Arrays. Genechip Operating Software v1.3 (Affymetrix, South San Francisco, CA) was used to extract images and normalize chip data. All microarray data was analyzed using Genesifter software (Seattle, WA). To generate gene lists, log transformed data was compared between groups using Welch's *t* test with Bonferroni correction and median normalization. Quality was set at 1.0.

Acknowledgments

We thank Dr. Danbin Xu and YiJun Wang for real-time reverse transcription-PCR analysis, Dr. Tom Walsh and Melissa Wollan for PTEN sequencing, Dr. Ming Lee for help with microarray data analysis, and Dr. Peter Rabinovitch, Maria Bravo, and Jeanne Fredrickson for helpful discussions.

References

1. Risch HA, McLaughlin JR, Cole DE, et al. Prevalence and penetrance of germline BRCA1 and BRCA2 mutations in a population series of 649 women with ovarian cancer. Am J Hum Genet 2001;68:700–10.

2. Pal T, Permuth-Wey J, Betts JA, et al. BRCA1 and BRCA2 mutations account for a large proportion of ovarian carcinoma cases. Cancer 2005;104:2807–16.

3. Ford D, Easton DF, Stratton M, et al. Genetic heterogeneity and penetrance analysis of the BRCA1 and BRCA2 genes in breast cancer families. Am J Hum Genet 1998;62:676–89.

4. King MC, Marks JH, Mandell JB. Breast and ovarian cancer risks due to inherited mutations in BRCA1 and BRCA2. Science 2003;302:643–6.

5. Dinulescu DM, Ince TA, Quade BJ, Shafer SA, Crowley D, Jacks T. Role of K-ras and Pten in the development of mouse models of endometriosis and endometrioid ovarian cancer. Nat Med 2005;11:63–70.

6. Connolly DC, Bao R, Nikitin AY, et al. Female mice chimeric for expression of the simian virus 40 TAg under control of the MISIIR promoter develop epithelial ovarian cancer. Cancer Res 2003;63:1389–97.

7. Flesken-Nikitin A, Choi KC, Eng JP, Shmidt EN, Nikitin AY. Induction of carcinogenesis by concurrent inactivation of p53 and Rb1 in the mouse ovarian surface epithelium. Cancer Res 2003;63:3459–63.

8. Orsulic S, Li Y, Soslow RA, Vitale-Cross LA, Gutkind JS, Varmus HE. Induction of ovarian cancer by defined multiple genetic changes in a mouse model system. Cancer Cell 2002;1:53–62.

9. Venkitaraman AR. Cancer susceptibility and the functions of BRCA1 and BRCA2. Cell 2002;108:171–82.

10. Welcsh PL, King MC. BRCA1 and BRCA2 and the genetics of breast and ovarian cancer. Hum Mol Genet 2001;10:705–13.

11. Zhang J, Powell SN. The role of the BRCA1 tumor suppressor in DNA double-strand break repair. Mol Cancer Res 2005;3:531–9.

12. Deng CX. BRCA1: cell cycle checkpoint, genetic instability, DNA damage response and cancer evolution. Nucleic Acids Res 2006;34:1416–26.

13. Mullan PB, Quinn JE, Harkin DP. The role of BRCA1 in transcriptional regulation and cell cycle control. Oncogene 2006;25:5854–63.

14. Yuan Y, Kim WH, Han HS, et al. Establishment and characterization of human ovarian carcinoma cell lines. Gynecol Oncol 1997;66:378–87.

15. Indraccolo S, Tisato V, Agata S, et al. Establishment and characterization of xenografts and cancer cell cultures derived from BRCA1$^{-/-}$ epithelial ovarian cancers. Eur J Cancer 2006;42:1475–83.

16. Zhou BB, Elledge SJ. The DNA damage response: putting checkpoints in perspective. Nature 2000;408:433–9.

17. Karagiannis TC, El-Osta A. Double-strand breaks: signaling pathways and repair mechanisms. Cell Mol Life Sci 2004;61:2137–47.

18. Shiloh Y. ATM and ATR: networking cellular responses to DNA damage. Curr Opin Genet Dev 2001;11:71–7.

19. Bakkenist CJ, Kastan MB. DNA damage activates ATM through intermolecular autophosphorylation and dimer dissociation. Nature 2003;421:499–506.

20. Cortez D, Wang Y, Qin J, Elledge SJ. Requirement of ATM-dependent phosphorylation of brca1 in the DNA damage response to double-strand breaks. Science 1999;286:1162–6.

21. Morin PJ. Claudin proteins in human cancer: promising new targets for diagnosis and therapy. Cancer Res 2005;65:9603–6.

22. Oku N, Sasabe E, Ueta E, Yamamoto T, Osaki T. Tight junction protein claudin-1 enhances the invasive activity of oral squamous cell carcinoma cells by promoting cleavage of laminin-5 gamma2 chain via matrix metalloproteinase (MMP)-2 and membrane-type MMP-1. Cancer Res 2006;66:5251–7.

23. Scully R, Ganesan S, Vlasakova K, Chen J, Socolovsky M, Livingston DM. Genetic analysis of BRCA1 function in a defined tumor cell line. Mol Cell 1999; 4:1093–9.

24. Wilson CA, Ramos L, Villasenor MR, et al. Localization of human BRCA1 and its loss in high-grade, non-inherited breast carcinomas. Nat Genet 1999;21: 236–40.

25. Orban TI, Olah E. Emerging roles of BRCA1 alternative splicing. Mol Pathol 2003;56:191–7.

26. Wang H, Shao N, Ding QM, Cui J, Reddy ES, Rao VN. BRCA1 proteins are transported to the nucleus in the absence of serum and splice variants BRCA1a, BRCA1b are tyrosine phosphoproteins that associate with E2F, cyclins and cyclin dependent kinases. Oncogene 1997;15:143–57.

27. Thakur S, Zhang HB, Peng Y, et al. Localization of BRCA1 and a splice variant identifies the nuclear localization signal. Mol Cell Biol 1997;17:444–52.

28. Scully R, Chen J, Ochs RL, et al. Dynamic changes of BRCA1 subnuclear location and phosphorylation state are initiated by DNA damage. Cell 1997;90: 425–35.

29. Zhang J, Willers H, Feng Z, et al. Chk2 phosphorylation of BRCA1 regulates DNA double-strand break repair. Mol Cell Biol 2004;24:708–18.

30. Hartwell LH, Weinert TA. Checkpoints: controls that ensure the order of cell cycle events. Science 1989;246:629–34.

31. Kuerbitz SJ, Plunkett BS, Walsh WV, Kastan MB. Wild-type p53 is a cell cycle checkpoint determinant following irradiation. Proc Natl Acad Sci U S A 1992;89:7491–5.

32. Xu B, Kim S, Kastan MB. Involvement of Brca1 in S-phase and G(2)-phase checkpoints after ionizing irradiation. Mol Cell Biol 2001;21:3445–50.

33. Xu B, O'Donnell AH, Kim ST, Kastan MB. Phosphorylation of serine 1387 in Brca1 is specifically required for the Atm-mediated S-phase checkpoint after ionizing irradiation. Cancer Res 2002;62:4588–91.

34. Young BR, Painter RB. Radioresistant DNA synthesis and human genetic diseases. Hum Genet 1989;82:113–7.

35. Juan G, Traganos F, James WM, et al. Histone H3 phosphorylation and expression of cyclins A and B1 measured in individual cells during their progression through G_2 and mitosis. Cytometry 1998;32:71–7.

36. Abraham RT. Cell cycle checkpoint signaling through the ATM and ATR kinases. Genes Dev 2001;15:2177–96.

37. Wang Y, Cortez D, Yazdi P, Neff N, Elledge SJ, Qin J. BASC, a super complex of BRCA1-associated proteins involved in the recognition and repair of aberrant DNA structures. Genes Dev 2000;14:927–39.

38. Ben David Y, Chetrit A, Hirsh-Yechezkel G, et al. Effect of BRCA mutations on the length of survival in epithelial ovarian tumors. J Clin Oncol 2002;20:463–6.

39. Cass I, Baldwin RL, Varkey T, Moslehi R, Narod SA, Karlan BY. Improved survival in women with BRCA-associated ovarian carcinoma. Cancer 2003;97: 2187–95.

40. Boyd J, Sonoda Y, Federici MG, et al. Clinicopathologic features of BRCA-linked and sporadic ovarian cancer. JAMA 2000;283:2260–5.

41. Husain A, He G, Venkatraman ES, Spriggs DR. BRCA1 up-regulation is associated with repair-mediated resistance to *cis*-diamminedichloroplatinum(II). Cancer Res 1998;58:1120–3.

42. Bhattacharyya A, Ear US, Koller BH, Weichselbaum RR, Bishop DK. The breast cancer susceptibility gene BRCA1 is required for subnuclear assembly of Rad51 and survival following treatment with the DNA cross-linking agent cisplatin. J Biol Chem 2000;275:23899–903.

43. Quinn JE, Kennedy RD, Mullan PB, et al. BRCA1 functions as a differential modulator of chemotherapy-induced apoptosis. Cancer Res 2003;63:6221–8.

44. Cannistra SA. Cancer of the ovary. N Engl J Med 2004;351:2519–29.

45. Staff S, Nupponen NN, Borg A, Isola JJ, Tanner MM. Multiple copies of mutant BRCA1 and BRCA2 alleles in breast tumors from germ-line mutation carriers. Genes Chromosomes Cancer 2000;28:432–42.

46. Tomlinson GE, Chen TT, Stastny VA, et al. Characterization of a breast cancer cell line derived from a germ-line BRCA1 mutation carrier. Cancer Res 1998;58:3237–42.

47. Abbott DW, Thompson ME, Robinson-Benion C, Tomlinson G, Jensen RA, Holt JT. BRCA1 expression restores radiation resistance in BRCA1-defective cancer cells through enhancement of transcription-coupled DNA repair. J Biol Chem 1999;274:18808–12.

48. Yarden RI, Pardo-Reoyo S, Sgagias M, Cowan KH, Brody LC. BRCA1 regulates the G_2/M checkpoint by activating Chk1 kinase upon DNA damage. Nat Genet 2002;30:285–9.

49. Yamane K, Chen J, Kinsella TJ. Both DNA topoisomerase II-binding protein 1 and BRCA1 regulate the G_2-M cell cycle checkpoint. Cancer Res 2003;63: 3049–53.

50. Yu X, Chini CC, He M, Mer G, Chen J. The BRCT domain is a phospho-protein binding domain. Science 2003;302:639–42.

51. Zhong Q, Chen CF, Chen PL, Lee WH. BRCA1 facilitates microhomology-mediated end joining of DNA double strand breaks. J Biol Chem 2002;277: 28641–7.

52. Merel P, Prieur A, Pfeiffer P, Delattre O. Absence of major defects in non-homologous DNA end joining in human breast cancer cell lines. Oncogene 2002; 21:5654–9.

53. Bau DT, Fu YP, Chen ST, et al. Breast cancer risk and the DNA double-strand break end-joining capacity of nonhomologous end-joining genes are affected by BRCA1. Cancer Res 2004;64:5013–9.

54. Usami Y, Chiba H, Nakayama F, et al. Reduced expression of claudin-7 correlates with invasion and metastasis in squamous cell carcinoma of the esophagus. Hum Pathol 2006;37:569–77.

55. Nagaraja GM, Othman M, Fox BP, et al. Gene expression signatures and biomarkers of noninvasive and invasive breast cancer cells: comprehensive profiles by representational difference analysis, microarrays and proteomics. Oncogene 2006;25:2328–38.

56. Quan C, Lu SJ. Identification of genes preferentially expressed in mammary epithelial cells of Copenhagen rat using subtractive hybridization and micro-arrays. Carcinogenesis 2003;24:1593–9.

57. Ishikawa K, Nagase T, Nakajima D, et al. Prediction of the coding sequences of unidentified human genes. VIII. 78 new cDNA clones from brain which code for large proteins *in vitro*. DNA Res 1997;4:307–13.

58. Andrews HN, Mullan PB, McWilliams S, et al. BRCA1 regulates the interferon gamma-mediated apoptotic response. J Biol Chem 2002;277: 26225–32.

59. Jazaeri AA, Yee CJ, Sotiriou C, Brantley KR, Boyd J, Liu ET. Gene expression profiles of BRCA1-linked, BRCA2-linked, and sporadic ovarian cancers. J Natl Cancer Inst 2002;94:990–1000.

60. Yang Y, Lee JH, Kim KY, et al. The interferon-inducible 9–27 gene modulates the susceptibility to natural killer cells and the invasiveness of gastric cancer cells. Cancer Lett 2005;221:191–200.

61. Asefa B, Klarmann KD, Copeland NG, Gilbert DJ, Jenkins NA, Keller JR. The interferon-inducible p200 family of proteins: a perspective on their roles in cell cycle regulation and differentiation. Blood Cells Mol Dis 2004; 32:155–67.

62. Sen GC. Novel functions of interferon-induced proteins. Semin Cancer Biol 2000;10:93–101.

63. Ziv Y, Bar-Shira A, Pecker I, et al. Recombinant ATM protein complements the cellular A-T phenotype. Oncogene 1997;15:159–67.

64. Nellemann C, Vinggaard AM, Dalgaard M, Hossaini A, Larsen JJ. Quantification of antiandrogen effect determined by Lightcycler technology. Toxicology 2001;163:29–38.

65. Schreiber E, Matthias P, Muller MM, Schaffner W. Rapid detection of octamer binding proteins with 'mini-extracts', prepared from a small number of cells. Nucleic Acids Res 1989;17:6419.

66. Rabinovitch PS, Reid BJ, Haggitt RC, Norwood TH, Rubin CE. Progression to cancer in Barrett's esophagus is associated with genomic instability. Lab Invest 1989;60:65–71.

67. Jaspers NGJ, Zdzienicka MZ. Inhibition of DNA synthesis by ionizing radiation. In: Henderson DS, Henderson DS. DNA repair protocols: eukaryotic Systems. Totowa (NJ): Humana Press; 1999. p. 535–42.